Vision Research 49 (2009) 1765–1774

Contents lists available at ScienceDirect

Vision Research

journal homepage: www.elsevier.com/locate/visres

Binocular properties of curvature-encoding mechanisms revealed through two shape after-effects

Elena Gheorghiu *, Frederick A.A. Kingdom, Minh-Thu Thai, Lavanya Sampasivam

McGill Vision Research, Department of Ophthalmology, McGill University, 687 Pine Avenue W., Montreal, Quebec, Canada H3A 1A1

ARTICLE INFO

Article history:
Received 16 December 2008
Received in revised form 12 February 2009

Keywords:
Binocular
Curvature
Interocular
Disparity
Adaptation
After-effect
Texture

ABSTRACT

We investigated the binocular properties of curvature-encoding mechanisms using the shape-frequency and shape-amplitude after-effects (or SFAE and SAAE). The SFAE and SAAE refer to the shifts observed in, respectively, the shape-frequency and shape-amplitude of a sinusoidal test contour following adaptation to a contour with different shape-frequency/shape-amplitude. We examined (i) the contribution of monocular versus binocular mechanisms to the SFAE and SAAE by measuring the interocular transfer of these after-effects, (ii) the stereo-depth selectivity of the after-effects and (iii) the depth selectivity of the reduction in the after-effects from texture-surround inhibition. Our results reveal that (i) both SFAE and SAAE have a high degree of interocular transfer (on average >90%), suggesting that they are mediated primarily by binocular mechanisms, (ii) neither SFAE nor SAAE are selective to stereo-defined depth and (iii) the reduction in the SFAE and SAAE from texture-surround inhibition is selective for stereo-depth. We conclude that the SFAE and SAAE are mediated by binocularly driven curvature-selective neurons that are not disparity selective in themselves but which receive inputs from neurons that are subject to depth- and orientation-selective texture-surround inhibition.

1. Introduction

Several studies have revealed that shape encoding mechanisms are located at various levels in the visual cortex, from oriented line and edge detectors in V1 (DeValois & DeValois, 1988; Hubel & Wiesel, 1968; Wilson, 1991), to curvature-sensitive detectors in V1 and V2 (Koenderink & Richards, 1988; Wilson & Richards, 1989), to parts-of-shape detectors in V4 (Gallant, Braun, & van Essen, 1993; Gallant, Connor, Rakshit, Lewis, & van Essen, 1996; Habak, Wilkinson, Zahker, & Wilson, 2004; Keeble & Hess, 1999; Levi & Klein, 2000; Pasupathy & Connor, 2002; Regan & Hamstra, 1992) and finally to whole-shape detectors in IT and LOC (Gross, 1992; Ito, Fujita, Tamura, & Tanaka, 1994; Tanaka, 1996).

In this communication we provide new psychophysical evidence concerning the binocular properties of the mechanisms encoding contour curvature. Although numerous studies have examined curvature-encoding mechanisms, one issue that has not been addressed is whether curvature-encoding is mediated by monocular or binocular mechanisms. It is well established that neurons in the primary visual cortex (V1), where the left and right eyes' signals converge, show various degrees of binocularity, from completely monocular to completely binocular (Hubel & Wiesel, 1962, 1968). Neurophysiological recordings from neurons in areas beyond V1 have shown that a large proportion of neurons in areas V2, V3, V4 and MT are binocular (Felleman & van Essen, 1987; Kaskan, Lu, Dillenburger, Kaas, & Roe, 2008; Maunsell & van Essen, 1983; Shipp & Zeki, 2002; Zeki, 1978). Several studies report that very few MT (Maunsell & van Essen, 1983) and IT (Janssen, Vogels, & Orban, 2000a, 2000b; Uka, Tanaka, Yoshiyama, Kato, & Fujita, 2000) neurons are driven monocularly; thus for higher visual areas binocularity appears to be the rule. If curvature is encoded at the earlier stages in cortical processing, then some or even all the mechanisms could be monocular, whereas if curvature is encoded at a relatively late stage of cortical processing then the mechanisms will almost certainly be binocular. One aim of the present study is to determine the relative importance of monocular and binocular curvature-encoding mechanisms.

We use the term 'encoding' to refer to mechanisms that *represent* rather than *discriminate* curvature. We have argued previously that curvature discrimination is probably mediated by mechanisms different to those mediating curvature representation (Gheorghiu & Kingdom, 2007a, 2008, 2009). Specifically we have argued that curvature discrimination likely involves relatively simple neural machinery, such as end-stopped neurons (Dobbins, Zucker, & Cynader, 1987, 1989) or neurons that compare responses from two orientation-selective V1 simple cells positioned at different points along the curve (Anzai, Peng, & van Essen, 2007; Hedge & van Essen, 2000; Kramer & Fahle, 1996; Tyler, 1973; Wilson, 1985; Wilson & Richards, 1989). However the representation of

* Corresponding author.
E-mail address: elena.gheorghiu@mcgill.ca (E. Gheorghiu).

0042-6989/$ - see front matter © 2009 Elsevier Ltd. All rights reserved.
doi:10.1016/j.visres.2009.04.010

curvature probably involves more complex neural machinery, perhaps neurons receiving inputs from a set of orientation-selective units whose receptive fields are arranged along a curve (Gheorghiu & Kingdom, 2009; Poirier & Wilson, 2006). The issue of curvature representation versus curvature detection/discrimination has been addressed in more detail elsewhere (Gheorghiu & Kingdom, 2009).

An important tool in the study of shape representation is the shape after-effect, the phenomenon in which the perceived shape of an object is altered following adaptation to a slightly different shape (Anderson, Habak, Wilkinson, & Wilson, 2007; Blakemore & Over, 1974; Gheorghiu & Kingdom, 2007a, 2007b, 2008; Hancock & Peirce, 2008; Regan & Hamstra, 1992; Suzuki, 2001, 2003; Suzuki & Cavanagh, 1998). Two shape after-effects, the shape-frequency and shape-amplitude after-effects, or SFAE and SAAE, have been recently used to study the visual coding of curvature (Gheorghiu & Kingdom, 2007a, 2007b, 2008). The SFAE and SAAE are the perceived shifts in, respectively, the shape-frequency and shape-amplitude of a sinusoidal test contour following adaptation to a sinusoidal contour of slightly different shape-frequency/shape-amplitude. We have shown that the SFAEs/SAAEs are mediated by mechanisms that encode curvature, rather than local orientation, periodicity, luminance spatial-frequency, position and global shape. However, the relative contribution of monocular versus binocular mechanisms to the SFAE/SAAE is at present unknown.

To examine whether the SFAE and SAAE are mediated by primarily monocular or primarily binocular mechanisms, we have measured the amount of their interocular transfer. Interocular transfer refers to the relative size of the after-effect when the adaptor and test are presented to opposite eyes compared to when presented to the same eyes. An interocular transfer of 100% means that the different-eye and same-eye after-effects are of the same magnitude, and is indicative of a purely binocular process (Blake, Overton, & Lema-Stern, 1981; Moulden, Patterson, & Swanson, 1998). An interocular transfer that is small (e.g. <50%) suggests that the mechanisms involved are primarily monocular. Intermediate levels of interocular transfer are best explained in terms of a mixture of monocular and binocular mechanisms, perhaps implying processing in low-level visual areas where the range of binocularity is mixed (Moulden, 1980; Moulden et al., 1998). Interocular transfers greater than 100% reflect simultaneous adaptation of both partly monocular and completely binocular high-level neurons (Nishida & Ashida, 2001). Examples of measured interocular transfers include 40–60% for the tilt after-effect (Paradiso, Shimojo, & Nakayama, 1989), 50–70% for the size after-effect (Bjørklund & Magnussen, 1981; Blake et al., 1981), 70–100% for the motion after-effect (Moulden et al., 1998; Nishida, Ashida, & Sato, 1994; Raymond, 1993; Steiner, Blake, & Rose, 1994), 100–1000% for the flicker-motion after-effect (Nishida & Ashida, 2001) and about 75% for the global-form after-effect obtained with Glass patterns (Vreven & Berge, 2007). However, to our knowledge no study has investigated interocular transfer for curvature after-effects.

If at least some curvature-encoding mechanisms are binocular then this raises the possibility that the mechanisms are tuned, or selective for retinal disparity and hence stereoscopic-depth. Recent neurophysiological studies have shown that disparity-selective neurons in area IT are also selective for shape (Uka et al., 2000). Tanaka, Uka, Yoshiyama, Kato, and Fijita (2001) found that IT neurons responded to shapes defined solely by binocular disparity. Disparity-tuned neurons are also found in area V4 (DeYoe & van Essen, 1985; Hinkle & Connor, 2001, 2002, 2005; Watanabe, Tanaka, Uka, & Fujita, 2002), an area known to be involved in curvature and object representation (Pasupathy & Connor, 1999, 2001, 2002). However, no neurophysiological or behavioral studies have examined directly the effects of binocular disparity on the encoding of curvature.

Recently, Kingdom and Prins (2009, 2005) found that the SFAE for a single contour test was roughly halved when the adaptor contour was surrounded by parallel but not orthogonal texture orientations. This phenomenon, called texture-surround inhibition, suggests that contours and textures interact in the brain in an important way. It is well known that a sub-set of V1 neurons that are sensitive to lines of a particular orientation are suppressed by oriented lines placed outside of their classical receptive field (Blakemore & Tobin, 1972; Cavanaugh, Bair, & Movshon, 1997; Jones, Grieve, Wang, & Sillito, 2001; Knierim & van Essen, 1992; Levitt & Lund, 1997; Nelson & Frost, 1978; Nothdurft, Gallant, & van Essen, 1999; Yao & Li, 2002). The suppression is maximal when the orientations are the same as the preferred orientation of the neuron, and minimal when the orientations are orthogonal to the preferred orientation of the neuron. These V1 neurons are said to exhibit '*iso-orientation surround suppression*' or IOSS. Almost 80% of the orientation-selective V1 neurons exhibit IOSS. Petkov and Westenberg (2003) and Grigorescu, Petkov, and Westenberg (2004) have simulated the responses of these neurons to natural scenes and found them to be sensitive to isolated contours, such as the edges of objects, but relatively unresponsive to lines in dense textures. Kingdom and Prins (2009) argued that the orientation-selective texture-surround inhibition they demonstrated with SFAE was probably a manifestation of IOSS, and therefore that IOSS neurons in area V1 feed their responses into shape-encoding neurons in higher visual areas. They also showed that texture-surround inhibition of the SFAE was not a result of the disruption of 'good continuity' in the central adapting contour or due to a reduction in the degree to which it 'popped-out'. Kingdom and Prins (2009) concluded that texture-surround inhibition is directly involved in contour-shape coding. Besides the importance of local orientation however, little is known about the properties of texture-surround inhibition.

In this study we consider what happens when the inhibitory texture-surround is placed in a different stereo-depth plane to that of the central adaptor contour. If the SFAE/SAAE is unchanged, this suggests that texture-surround inhibition is agnostic to stereo-depth. However if the SFAE/SAAE increases to the level obtained with no texture-surround, this suggests that texture-surround inhibition is selective to stereo-depth.

To summarize: we have investigated the relative involvement of monocular versus binocular mechanisms in curvature-encoding by measuring (i) interocular transfer of the SFAE/SAAE, (ii) stereo-depth-selectivity of the SFAE/SAAE and (iii) stereo-depth-selectivity of texture-surround inhibition. A large amount of interocular transfer would suggest that the after-effects are mediated primarily by binocular mechanisms located beyond V1, whereas a small amount of interocular transfer would suggest that the after-effects are mediated primarily by monocular mechanisms in V1. If the after-effects are significantly greater when the adaptors and tests are positioned in the same compared to different stereo-depth planes, this suggests that curvature-encoding mechanisms are selective for stereo-depth. Finally, if the reduction in after-effect from texture-surround inhibition is eliminated when the adaptor contour and texture-surround are placed in different stereo-depth planes, this suggests that texture-surround inhibition is selective for stereo-depth.

Readers who are able to free-fuse may experience same-depth adaptor/test versions of the SFAE and the SAAE in Fig. 1a and b, by first moving their eyes back and forth along the horizontal markers on the left for about a minute, and then transferring their gaze to the central spot on the right. The two test contours, which are identical, should appear different in shape-frequency or shape-amplitude. Both after-effects survive shape-phase randomization during adaptation, as can be experienced in the flat, non-static-adaptor versions on http://www.mvr.mcgill.ca/Fred/research.htm#contourShapePerception.

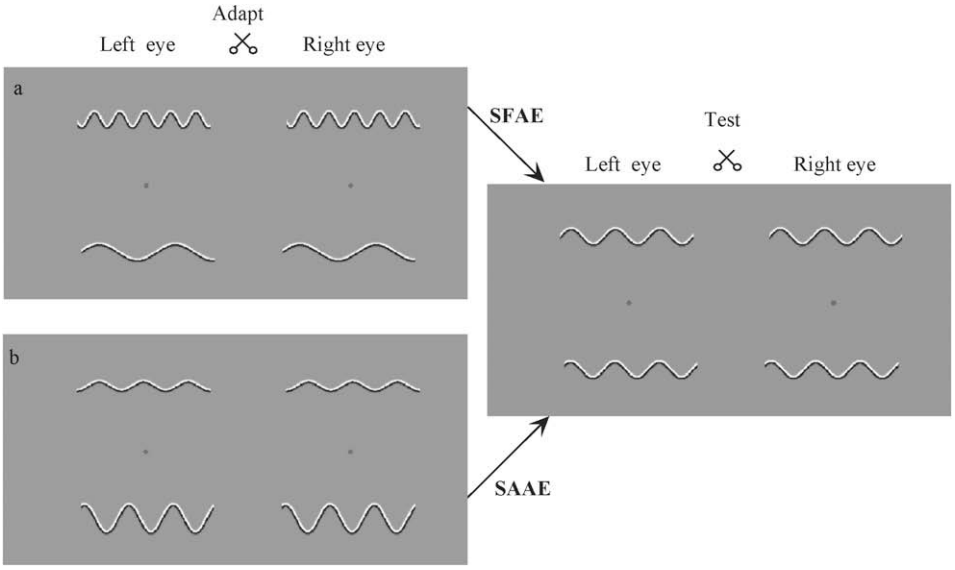

Fig. 1. Stimuli used in the experiments. The contour-shape stimuli can be viewed stereoscopically by cross fusing the left and right eye's images. One can experience (a) the shape-frequency after-effect (SFAE) and (b) the shape-amplitude after-effect (SAAE) by moving one's eyes back and forth along the markers located midway between the pair of adapting contours (left) for about 90 s, and then shifting one's gaze to the middle of the test contours (right). The two test contours, which are identical, should appear different in shape-frequency or shape-amplitude.

2. General methods

2.1. Observers

Six subjects with normal or corrected-to-normal visual acuity and good stereoscopic vision participated in different experiments. Two of them (EG and FK) were experienced stereoscopic observers.

2.2. Stimuli

The stimuli were generated by a VSG2/5 video-graphics card (Cambridge Research Systems) with 12-bits contrast resolution, presented on a calibrated, gamma-corrected Sony Trinitron monitor, running at 120 Hz frame rate and with a spatial resolution of 1024×768 pixels. The mean luminance of the monitor was 40 cd/m^2. The two stereo-halves were presented on either side of the monitor screen separated by 3.75° and combined optically by a modified 8-mirror Wheatstone stereoscope. All mirrors were cemented into position except for the two front mirrors whose position along the line of sight of the subject could be adjusted until fusion was accomplished. Viewing distance, as measured by the length of the path of light from the monitor screen to the eyes was 105 cm. The mean luminance as measured through the stereoscope was 34 cd/m^2.

Example stereoscopic stimuli are shown in Fig. 1. Adaptation and test stimuli consisted of pairs of sine-wave-shaped contours. Unless otherwise stated, the adaptor pair for the SFAE consisted of contours with a shape-amplitude of 0.43° and shape frequencies of 0.25 and 0.75 c/deg, giving a geometric mean shape-frequency of 0.43 c/deg. For the SAAE, the shape-frequency of the adaptor pair was 0.43 c/deg, while the shape-amplitudes were 0.25° and 0.75°, giving a geometric mean shape-amplitude of 0.43°. The two adaptors and tests stereo-halves were presented on either side of the monitor screen at 3.5° above and below the fixation marker. The cross-sectional luminance profile of the contours was odd-symmetric and was generated according to a first derivative of a Gaussian function:

$$L(d) = L_{\text{mean}} \pm L_{\text{mean}} \cdot C \cdot \exp(0.5) \cdot (d/\sigma) \cdot \exp[-(d^2)/(2\sigma^2)] \qquad (1)$$

'where d is the distance from the midpoint of the contour's luminance profile along a line perpendicular to the tangent, L_{mean} mean luminance of 40 cd/m^2, C contrast and σ the space-constant. Unless otherwise stated, contrast C was set to 0.5 and σ to 0.044°. The $\pm$ sign determined the polarity of the contour. Our contours were designed to have a constant cross-sectional width, and the method used to achieve this is described in Gheorghiu and Kingdom (2006).

2.3. Procedure

Each session began with an initial adaptation period of 90 s, followed by a repeated test of 0.5 s duration interspersed with top-up adaptation periods of 2.5 s. During the adaptation period, the shape-phase of the contour was randomly changed every 0.5 s in order to prevent the formation of afterimages and to minimize the effects of local orientation adaptation. The presentation of the test contour was signaled by a tone. The shape-phase of the test contour was also randomly assigned in every test period. Subjects were required to fixate on the marker placed between each pair of contours for the entire session.

A staircase method was used to estimate the PSE. For the SFAE the geometric mean shape-frequency of the two test contours was held constant at 0.43 c/deg while the computer varied the relative shape-frequencies of the two tests in accordance with the subject's response. At the start of the test period the ratio of the two test shape-frequencies was set to a random number between 0.71 and 1.4. On each trial subjects indicated via a button press whether the upper or lower test contour had the higher perceived shape-frequency. The computer then changed the ratio of test shape-frequencies by a factor of 1.06 for the first five trials and 1.015 thereafter, in a direction opposite to that of the response, i.e. towards the PSE. The session was terminated after 25 trials. Six measurements were made for each condition, three in which the upper adaptor had the higher shape-frequency and three in which the lower adaptor had the higher shape-frequency. The shape-frequency ratio at the PSE was calculated as the geometric mean shape-frequency ratio of the test that followed the adaptor with the lower shape-frequency to the test that followed the adaptor

with the higher shape-frequency, averaged across the last 20 trials. In addition we measured for each condition the shape-frequency ratio at the PSE in the absence of the adapting stimulus (the no-adaptor condition). To obtain an estimate of the size of the SFAE we calculated the difference between the log with-adaptor shape-frequency ratio at the PSE and the mean log no-adaptor shape-frequency ratio at the PSE, for each with-adaptor measurement. We then calculated the mean and standard error of the differences across measurements and these are the values shown in the graphs.

The procedure for measuring the SAAE followed the same principle as for the SFAE. The computer varied the relative shape-amplitudes of the two tests in accordance with the subject's response, while the geometric mean shape-amplitude of the two test contours was held constant at 0.43°.

3. Experiments and results

3.1. Experiment 1: interocular transfer of curvature-encoding

In this experiment we examine the monocular versus binocular properties of curvature-encoding mechanisms by measuring interocular transfer of the SFAE and SAAE. This will tell us whether curvature-selective mechanisms are purely monocular, purely binocular or a combination of both monocular and binocular.

We used adaptor and test sine-wave-shaped contours presented (i) binocularly, (ii) monocularly to the left or to the right eye and (iii) interocularly. For the interocular presentation, the adaptor was presented to one eye, and the test to the other eye. The fixation marker was always presented binocularly. The magnitude of interocular transfer was defined as the log shape-frequency (or shape-amplitude) ratio obtained under the interocular condition divided by the log shape-frequency (or shape-amplitude) ratio obtained under the monocular condition. This definition is similar to that used for the measurement of motion-after-effect nulling strength by Nishida and Ashida (2000).

Fig. 2 shows SFAEs and SAAEs for binocular (black bars), monocular (light gray bar) and interocular (dark gray bars) adaptor-test conditions. The results indicate that SFAEs/SAAEs are slightly lower for the interocular condition in some conditions and some subjects. Fig. 3 shows the interocular transfer for SFAE (Fig. 3a) and SAAE (Fig. 3b). For each individual subject, the interocular transfer of the after-effects was larger than 80%. On average, the interocular transfer was 89.4% for SFAE and 95% for SAAE, indicating that the mechanisms mediating the SFAE and SAAE are located predominantly at the binocular level.

3.2. Experiment 2: stereo-depth selectivity of curvature-encoding

Here, we examine the stereo-depth selectivity of the SFAE and SAAE. If curvature mechanisms are selective for stereoscopic depth, we would expect the SFAE and SAAE to be reduced when the adaptor and test contours differ in stereo-depth.

Each pair of adapting and test contours consisted of one contour with +15′ (arcmin) crossed disparity and another contour with −15′ uncrossed disparity. This resulted in a depth separation of 30′ between the two contours. There were two contour arrangements: contour above fixation of +15′ and contour below fixation of −15′, and vice-versa. Example contours are shown in Fig. 1a and b. There were two adaptor-test conditions: (i) adaptor and test with the same depth sign and (ii) adaptor and test with different depth sign. A similar experiment was carried out for pairs of contours separated by 15′ in depth, that is one contour at +7.5′ crossed disparity and another contour at −7.5′ uncrossed disparity.

Fig. 4 shows the SFAE (Fig. 4a) and SAAEs (Fig. 4b) for same (light gray bars) and different (dark gray bars) adaptor-and-test depth-sign conditions for ±15′ (upper panels) and ±7.5′ (lower panels) disparity. The results show comparable size after-effects obtained with adaptor and test contours that have either the same or different depth-sign. A one-way ANOVA (analysis of variance) with Combination (same versus different stereo-depth) as factor, on both the SFAE and SAAE data showed that the effect of Combination was not significant (SFAE: $F(1) = 0.1538$, $p > 0.05$; SAAE: $F(1) = 0.21$; $p > 0.05$). These results offer no evidence that SFAEs and SAAEs are selective for stereo-depth.

3.3. Experiment 3: stereo-depth selectivity of texture-surround inhibition

Here we examine whether texture-surround inhibition of contour-shape encoding is selective to stereo-depth. The *adaptors* consisted of a central contour flanked by arrays of similar contours making a parallel-texture surround. Because a parallel-textured surround might narrow the luminance spatial-frequency bandwidth of the central contour the contours were constructed from Gabor patches which are narrowband, as in Kingdom and Prins (2009). The Gabors were odd-symmetric and hence d.c. balanced, with a spatial-frequency bandwidth of 1.5 octaves and center spatial frequency of 5 c/deg. The spacing between the Gabor patches along each contour was 0.4°. The orientation of each Gabor patch was collinear to the tangent of the curve of the contour, i.e. co-aligned with it. Example contours with and without texture-surrounds are shown in Fig. 5c–f. We used *three types* of adaptors: (i) a single central contour (Fig. 5a), (ii) a central contour flanked by surround contours in the same depth plane (Fig. 5b) and (iii) a central contour with surround contours in a different depth plane. In the last condition the disparity between center and surround contours was ±10′ (Fig. 5c and d). In all experiments the contour was in the plane of fixation and the texture was located 10′ either behind (see Fig. 5c) or in front of the contour (see Fig. 5d). For all three adaptation conditions, the *test* contours were always single contours consisting of Gabor patches those orientations were collinear to the tangent of the curve of the contour (see Fig. 5a). The test contours were always located at the same depth as the central contour of the adaptor.

The adaptor pair for the SFAE consisted of contours with a shape-amplitude of 0.35° and shape frequencies of 0.2 and 0.6 c/deg, giving a geometric mean shape-frequency of 0.35 c/deg. For the SAAE, the adaptor pair consisted of contours with a shape-frequency of 0.35 c/deg and shape-amplitudes of 0.2 and 0.6°, giving a geometric mean shape-amplitude of 0.35°.

Fig. 6 shows the SFAEs (Fig. 6a) and SAAEs (Fig. 6b) for contour-only (light gray bars), contour and surround in the same depth plane (white bars) and contour and surround in different depth planes (dark gray bars). There were no significant differences between the +10 and −10 disparity conditions, so the results were combined. The results show that while the presence of a same-depth surround reduces both after-effects, a different-depth surround has little effect (compare light and dark gray bars). To compare the reduction in the size of the after-effects between observers, we normalized the results to the single-contour-adaptor condition for each observer. Fig. 7a shows the average normalized results across observers for the SFAE (left) and SAAE (right). On average the after-effect is only 45% and 50% in the same-depth surround SFAE and SAAE, but 92% and 71%, respectively, with the different-depth surround. A one-way within-subjects ANOVA on the non-normalized data, Bonferroni corrected to allow for multiple comparisons, indicated that the three conditions (single-contour, same-depth-surround and different-depth-surround) were significantly different from each other ($F(2, 3) = 13.51$, $p < 0.05$

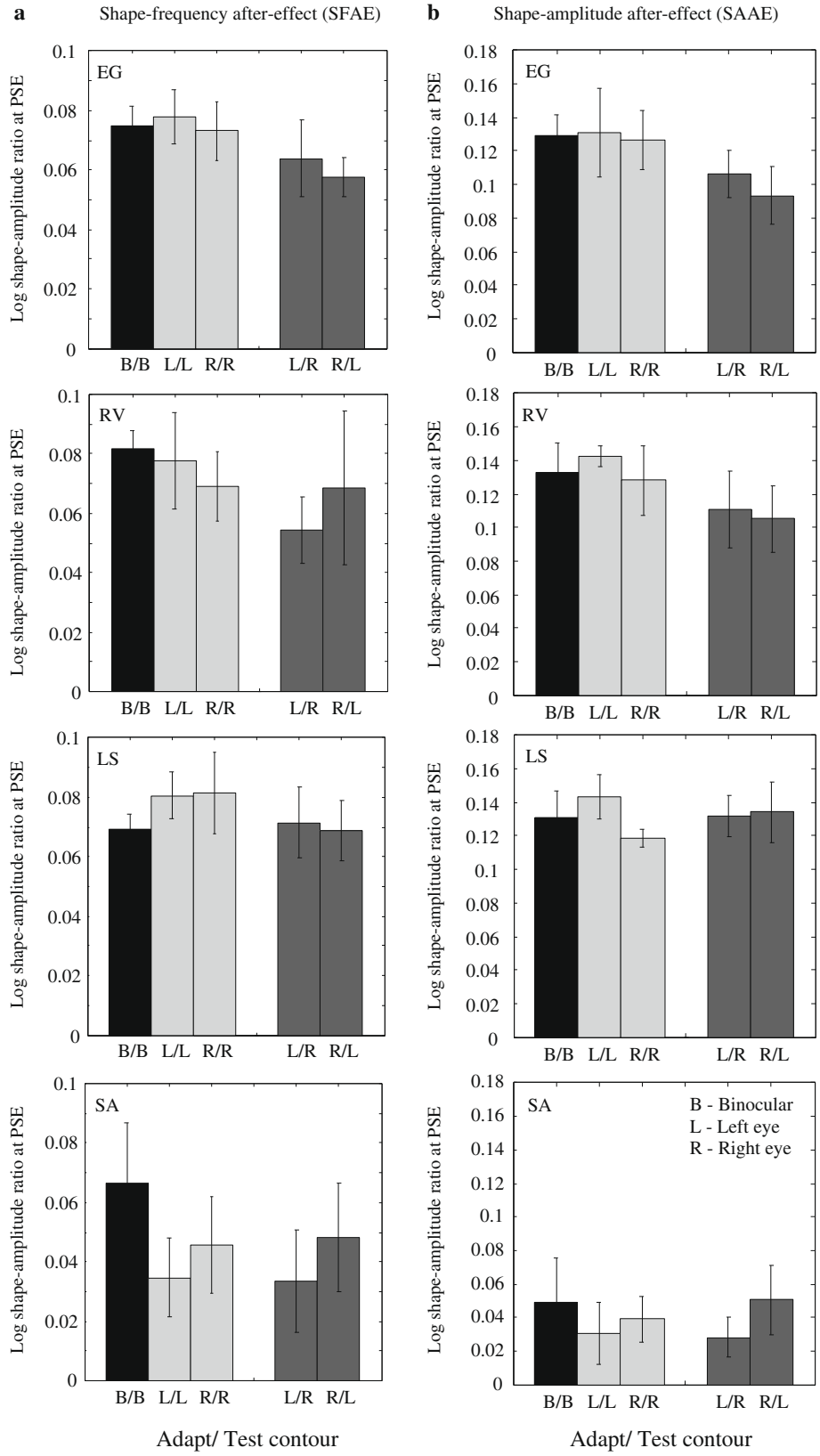

Fig. 2. Results for Experiment 1 – interocular transfer. (a) SFAEs and (b) SAAEs for binocular (black bars), monocular (light gray bar) and interocular (dark gray bars) adaptor–test conditions. Error bars represent standard errors of the mean difference between the with-adaptor and no-adaptor conditions calculated across six measurements.

for SFAE; $F(2, 3) = 62.16$, $p < 0.05$ for SAAE). All pair-wise comparisons were significantly different ($p < 0.05$) except for the single-contour versus different-depth conditions for the SFAE ($t = 1.076$, $p > 0.05$).

4. General discussion

We found that SFAEs and SAAEs (i) showed a high degree of interocular transfer (on average 89.4% for the SFAE and 95% for

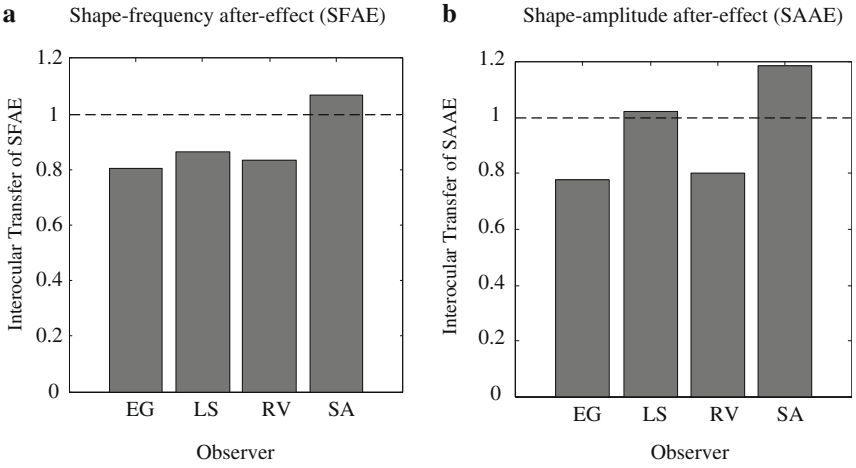

Fig. 3. Interocular transfer for (a) the SFAE and (b) SAAE, for four observers. The magnitude of interocular transfer was defined as the log shape-frequency, or shape-amplitude ratio obtained under the interocular condition divided by the log shape-frequency or shape-amplitude ratio obtained under the monocular condition. On average, the interocular transfer was 89.4% for SFAE and 95% for SAAE, indicating that the mechanisms mediating the SFAE and SAAE are located predominantly at the binocular level.

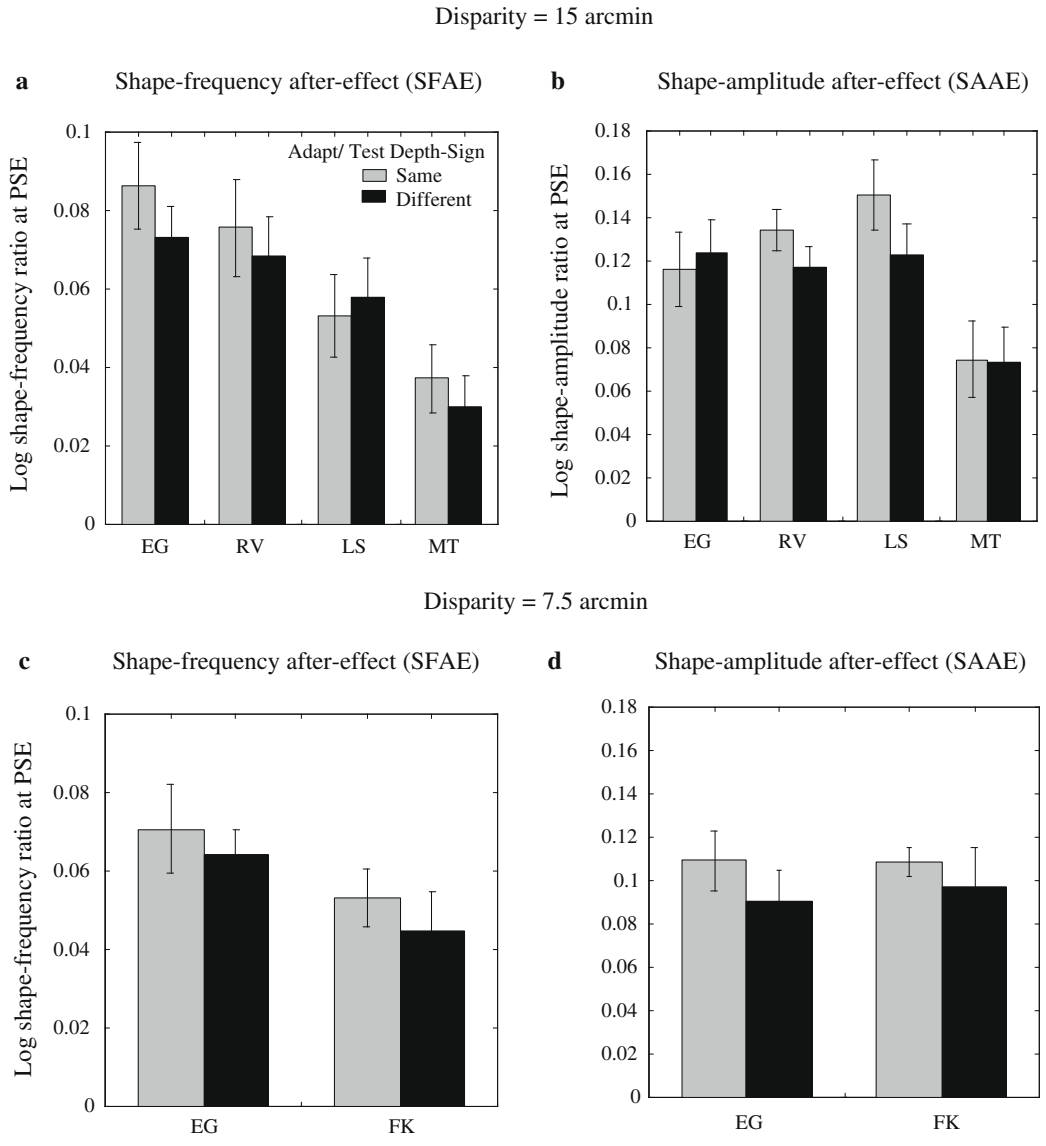

Fig. 4. Results for Experiment 2 – stereo-depth selectivity. (a) SFAEs and (b) SAAEs for same (light gray bars) and different (dark gray bars) adaptor-and-test depth-sign conditions for ±15′ (upper panels) and ±7.5′ (lower panels) disparity. Error bars are standard errors of the mean difference between the with-adaptor and no-adaptor conditions calculated across six measurements.

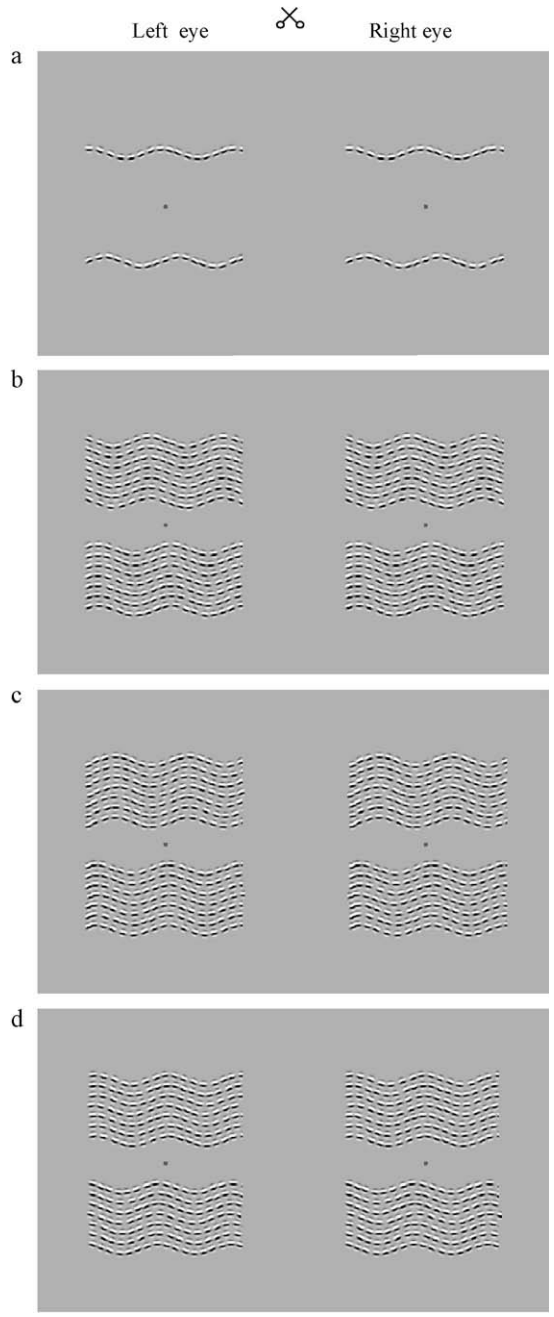

Fig. 5. Types of adaptors used in Experiment 3 – stereo-depth selectivity of texture-surround inhibition. (a) Single central contour; (b) central contour flanked by surround contours in the same depth plane and (c and d) central contour with surround contours in a different depth plane. The disparity between center and surround contours was ±10′. The parallel-texture surround could be located either (c) behind or (d) in front of the contour. In all conditions, the test contours were single contours consisting of Gabor patches those orientations were collinear to the tangent of the curve of the contour.

the SAAE), (ii) showed no selectivity to stereo-depth, but (iii) were selective to the stereo-depth of an inhibitory texture-surround.

A large amount of interocular transfer argues for a predominance of binocular mechanisms. Given our evidence that the SFAE/SAEE are mediated by curvature-sensitive mechanisms (Gheorghiu & Kingdom, 2007a, 2008) it follows that curvature-encoding mechanisms appear to be predominantly binocularly-driven. However the lack of selectivity to stereo-depth suggests that although binocularly-driven, curvature-encoding mechanisms are not tuned to disparity.

How does this square with the neurophysiology? A large number of studies have demonstrated that disparity-tuned neurons are found throughout the visual system, e.g. V1, V2, V3, V4 and MT (Cumming & Parker, 1999; Hinkle & Connor, 2001, 2002; Hinkle & Connor, 2005; Hubel & Livingstone, 1987; Maunsell & van Essen, 1983; Peterhans & von der Heydt, 1993; Prince, Cumming, & Parker, 2002; Prince, Pointon, Cumming, & Parker, 2002; Poggio & Fischer, 1977; Watanabe et al., 2002; Roy, Komatsu, & Wurtz, 1992). Other studies have shown that neurons in area V4 are involved in coding angles and curves (Pasupathy & Connor, 1999, 2001, 2002) as well as high-level shape information (Desimone & Schein, 1987; Kobatake & Tanaka, 1994; Gallant et al., 1993, 1996). Have any of these neurons been shown to be selective to *both* disparity and curvature? Hinkle and Connor (2001) recently tested 93 neurons in V4 that were stimulated by oriented bars (57 cells), angles (25 cells), circles (7 cells) and ellipses (4 cells). Of these, 80% were also selective for stereoscopic disparity. More recently, Hinkle and Connor (2005) found that V4 neurons were mainly stimulated by drifting oriented bars (409 from 452 neurons tested), were selective for disparity and that the degree of disparity-tuning was positively correlated with the degree of orientation- and color-tuning. Our negative finding with respect to the stereoscopic-depth tuning of the SFAE/SAAE appears at first sight to be inconsistent with the Hinkle and Connor (2001, 2005) findings. However the majority of V4 neurons in the Hinkle & Connor studies were stimulated with drifting oriented bars rather than curves, angles or simple shapes, so it is still possible that curvature-sensitive neurons in V4 are non-selective for disparity. Unfortunately to our knowledge there are no neurophysiological studies that have directly examined the selectivity to binocular disparity of neurons selective for curvature.

The results of our third experiment on the other hand indicate that contour-shape encoding mechanisms are primarily inhibited by parallel-texture-surrounds that lie in the same stereoscopic-depth plane. It is worth dwelling for a moment on this remarkable texture-surround-inhibition phenomenon. In the 'same-depth' condition, the parallel-surround adaptors (Fig. 5b) consisted of multiple contours covering most of the region of visual space containing the test contour, so one might expect the adaptive effect to be greater than that of a single-contour adaptor. However the opposite this is found; the SFAE and SAAE are reduced (compare white and light gray bars in Fig. 6). This forcefully demonstrates the impact that parallel-texture-surrounds have on contour-shape processing, and suggests that V1 neurons that exhibit IOSS feed their responses into those high-level visual areas that are directly involved in processing contour shape. The near-complete restoration of both after-effects when the adaptor's central contour and parallel-surround were positioned in different depth planes (compare dark and light gray bars in Fig. 6) implies that the disparities of the inhibitory extra-receptive field surrounds in IOSS neurons are the same as those of their classical receptive-field centers.

Although we are assuming here that IOSS operates in V1, it is possible that it also operates in higher visual areas. There is some evidence that in V4, neurons sensitive to oriented bars have a pronounced near-disparity bias (Hinkle & Connor, 2001, 2005; Watanabe et al., 2002), which Hinkle and Connor (2001, 2005) suggest might reflect their involvement in figure-ground segregation. It is possible therefore that these neurons might be subject to IOSS, and hence might mediate the results found here with texture-surrounds.

What other visual attributes besides disparity has texture-surround inhibition been found to be selective? Kingdom and Prins (2009) demonstrated that texture-surround inhibition is orientation-selective – hence the reason why we have referred to the inhibition as coming from parallel texture-surrounds. On the other hand Gheorghiu, Kingdom, and Varshney (2009) have recently

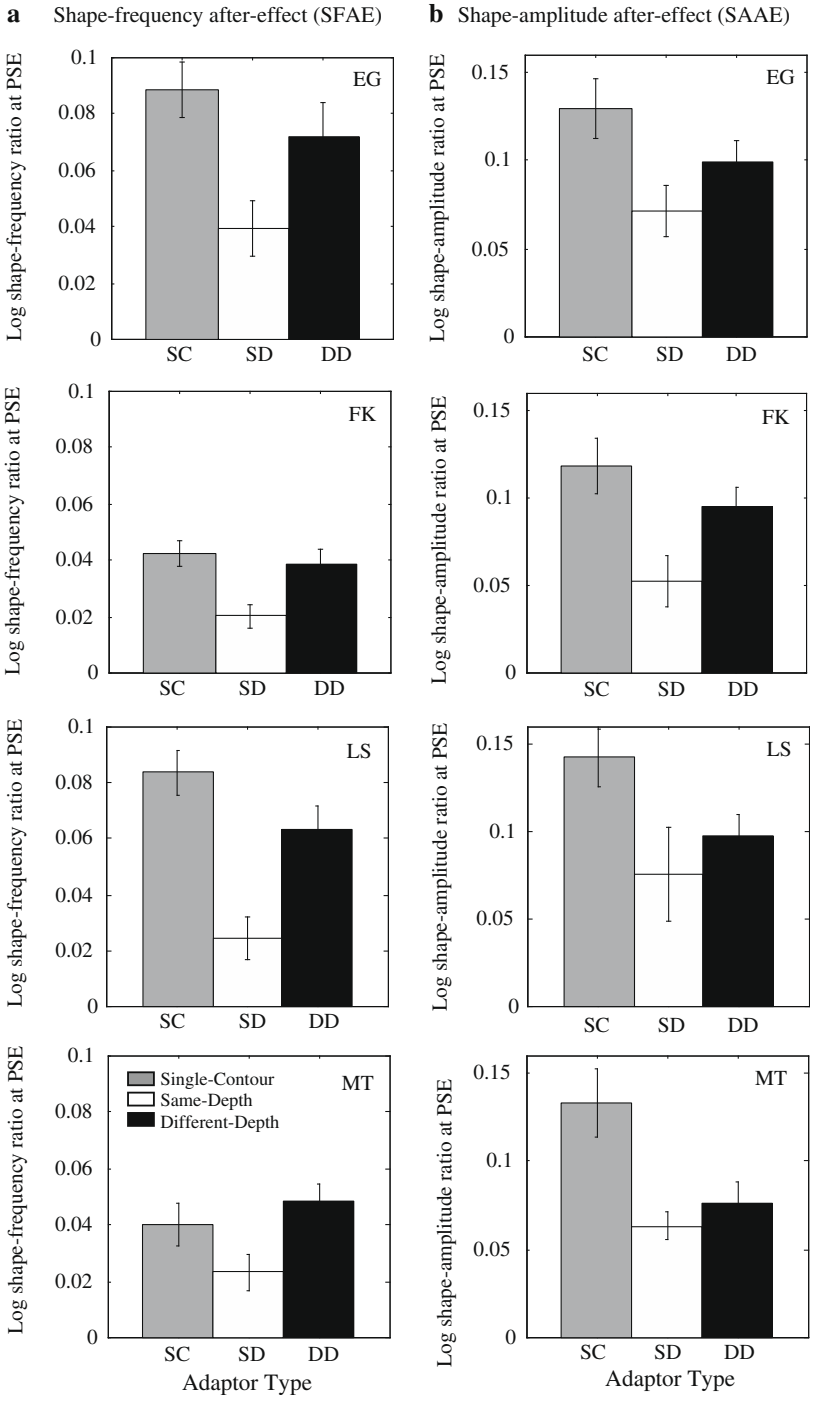

Fig. 6. Results for Experiment 3 – stereo-depth selectivity of texture-surround inhibition. (a) SFAEs and (b) SAAEs for contour-only (light gray bars), contour and surround in the same depth plane (white bars) and contour and surround in different depth planes (dark gray bars) conditions. Error bars are standard errors of the mean difference between the with-adaptor and no-adaptor conditions calculated across six measurements.

found that texture-surround inhibition does *not* appear to be selective for the direction of motion of the micropatterns in stimuli constructed from them. Further experiments are needed to elucidate further the properties of texture-surround inhibition of contour-shape coding.

Why then is contour-shape encoding itself not stereo-depth selective? If texture-surround inhibition accentuates isolated contours for subsequent shape analysis, it would make sense for the inhibition to be depth-selective in order that an isolated contour would not be inhibited by a texture lying in another depth plane. However when it comes to the analysis of contour-shape itself, depth information might be discarded in order to make shapes invariant to dimensions such as viewing angle and position in depth (Desimone, 1991; Kingdom, Field, & Olmos, 2007; Wallis & Rolls, 1997; Wiskott, 2004).

How therefore have the findings of this study advanced our knowledge of curvature processing? Since we find that curvature is encoded predominantly by binocular neurons, and hence most likely in higher visual areas, this reinforces the view that the mechanisms involved in representing curves are mediated by more complex, higher-level neural machinery than those involved in detecting and discriminating curves. In this regard the evidence

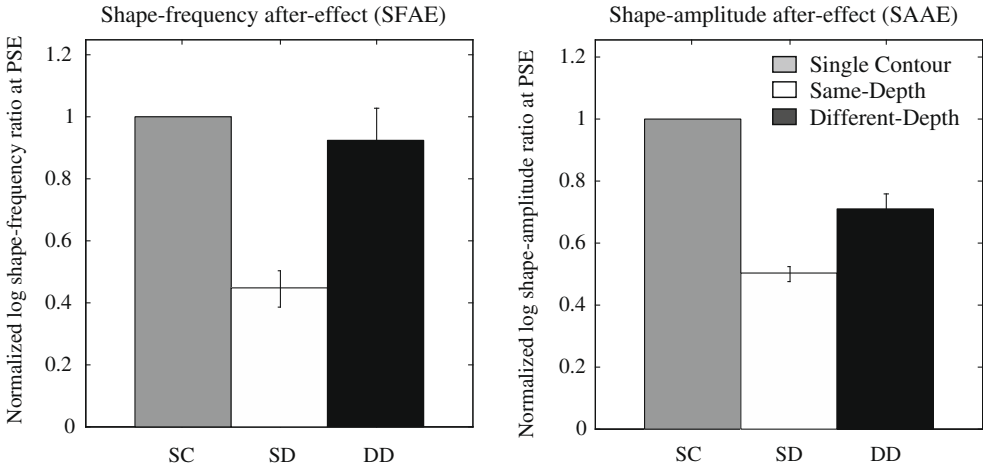

Fig. 7. The average normalized results across observers for the SFAE (left) and SAAE (right) for contour only (light gray bars), contour and surround in the same depth plane (white bars) and contour and surround in different depth planes (dark gray bars). Error bars are standard errors of the mean across observers. On average the SFAE is 45% and SAAE 50% in the same-depth surround condition, but 92% and 71%, respectively, in the different-depth surround condition.

from this study is consistent with the view that contour curvature is encoded by neurons that take as input V1 cells whose receptive fields are arranged in a curvilinear fashion. These afferent inputs to curvature-encoders are apparently orientation-selective (Gheorghiu & Kingdom, 2008) and multiplied (Gheorghiu & Kingdom, 2009).

Acknowledgments

This research was supported by a Natural Sciences and Engineering Research Council of Canada (NSERC) Grant # OGP01217130 and Canadian Institute of Health Research (CIHR) # MOP-11554 Grant given to F.K.

References

Anderson, N. D., Habak, C., Wilkinson, F., & Wilson, H. R. (2007). Evaluating shape after effects with radial frequency patterns. *Vision Research, 47*(3), 298–308.
Anzai, A., Peng, X., & van Essen, D. C. (2007). Neurons in monkey visual area V2 encode combinations of orientations. *Nature Neuroscience, 10*(10), 1313–1321.
Bjørklund, R. A., & Magnussen, S. (1981). A study of interocular transfer of spatial adaptation. *Perception, 10*(5), 511–518.
Blake, R., Overton, R., & Lema-Stern, S. (1981). Interocular transfer of visual aftereffects. *Journal of Experimental Psychology: Human Perception and Performance, 213*(1), 157–174.
Blakemore, C., & Over, R. (1974). Curvature detectors in human vision? *Perception, 3*(1), 3–7.
Blakemore, C., & Tobin, E. A. (1972). Lateral inhibition between orientation detectors in the cat's visual cortex. *Experimental Brain Research, 15*, 439–440.
Cavanaugh, J. R., Bair, W., & Movshon, J. A. (1997). Orientation-selective setting of contrast gain by the surrounds of macaque striate cortex neurons. *Neuroscience Abstracts, 23*, 227.
Cumming, B. G., & Parker, A. J. (1999). Binocular neurons in V1 of awake monkeys are selective for absolute, not relative, disparity. *Journal of Neuroscience, 19*, 5602–5618.
Desimone, R. (1991). Face-selective cells in the temporal cortex of monkeys. *Journal of Cognitive Neuroscience, 3*, 1–8.
Desimone, R., & Schein, S. J. (1987). Visual properties of neurons in area V4 of the macaque: sensititvity to stimulus form. *Journal of Neurophysiology, 57*(3), 835–868.
DeValois, R. L., & DeValois, K. K. (1988). *Spatial Vision*. Oxford University Press.
Dobbins, A., Zucker, S. W., & Cynader, M. S. (1987). Endstopping in the visual cortex as a substrate for calculating curvature. *Nature, 329*, 438–441.
Dobbins, A., Zucker, S. W., & Cynader, M. S. (1989). Endstopping and curvature. *Vision Research, 29*(10), 1371–1387.
DeYoe, E. A., & van Essen, D. C. (1985). Segregation of efferent connections and receptive field properties of visual area V2 of the macaque. *Nature, 317*, 58–61.
Felleman, D. J., & van Essen, D. C. (1987). Receptive field properties of neurons in area V3 of macaque monkey extrastriate cortex. *Journal of Neurophysiology, 57*(4), 889–920.
Gallant, J. L., Braun, J., & van Essen, D. C. (1993). Selectivity for polar, hyperbolic and Cartesian gratings in macaque visual cortex. *Science, 259*(5091), 100–103.
Gallant, J. L., Connor, C. E., Rakshit, S., Lewis, J. W., & van Essen, D. C. (1996). Neural responses to polar, hyperbolic, and Cartesian gratings in area V4 of the macaque monkey. *Journal of Neurophysiology, 76*(4), 2718–2739.
Gheorghiu, E., & Kingdom, F. A. A. (2009). Multiplication in curvature processing. *Journal of Vision, 9*(2): 23, 1–17.
Gheorghiu, E., & Kingdom, F. A. A., Varshney, R. (2009). Global not local motion direction tuning of curvature encoding mechanisms. *Journal of Vision, 9* [abstract] (in press).
Gheorghiu, E., & Kingdom, F. A. A. (2006). Luminance-contrast properties of contour-shape processing revealed through the shape-frequency after-effect. *Vision Research, 46*(21), 3603–3615.
Gheorghiu, E., & Kingdom, F. A. A. (2007a). The spatial feature underlying the shape-frequency and shape-amplitude after-effects. *Vision Research, 47*(6), 834–844.
Gheorghiu, E., & Kingdom, F. A. A. (2007b). Chromatic tuning of contour-shape mechanisms revealed through the shape-frequency and shape-amplitude after-effects. *Vision Research, 47*(14), 1935–1949.
Gheorghiu, E., & Kingdom, F. A. A. (2008). Spatial properties of curvature-encoding mechanisms revealed through the shape-frequency and shape-amplitude after-effects. *Vision Research, 48*(9), 1107–1124.
Grigorescu, C., Petkov, N., & Westenberg, M. A. (2004). Contour and boundary detection improved by surround suppression of texture edges. *Image and Vision Computing, 22*, 609–622.
Gross, C. G. (1992). Representation of visual stimuli in inferior temporal cortex. *Philosophical Transactions of the Royal Society of London Series B – Biological Sciences, 335*(1273), 3–10 [Review].
Habak, C., Wilkinson, F., Zahker, B., & Wilson, H. R. (2004). Curvature population coding for complex shapes in human vision. *Vision Research, 44*, 2815–2823.
Hancock, S., & Peirce, J. W. (2008). Selective mechanisms for simple contours revealed by compound adaption. *Journal of Vision, 8* (7): 11, 11–10.
Hedge, J., & van Essen, D. C. (2000). Selectivity for complex shapes in primate visual area V2. *Journal of Neuroscience, 20*(5), RC61.
Hinkle, D. A., & Connor, E. C. (2001). Disparity tuning in macaque area V4. *Neuroreport, 12*, 365–369.
Hinkle, D. A., & Connor, E. C. (2002). Three-dimensional orientation tuning in macaque area V4. *Nature Neuroscience, 5*, 665–670.
Hinkle, D. A., & Connor, E. C. (2005). Quantitative characterization of disparity tuning in ventral pathway area V4. *Journal of Neurophysiology, 94*, 2726–2737.
Hubel, D. H., & Livingstone, M. S. (1987). Segregation of form, color and stereopsis in primate area 18. *Journal of Neuroscience, 7*(11), 3378–3415.
Hubel, D. H., & Wiesel, T. N. (1962). Receptive fields, binocular interaction and functional architecture in the cat's visual cortex. *Journal of Physiology, 160*, 106–154 [London].
Hubel, D. H., & Wiesel, T. N. (1968). RFs and functional architecture of monkey striate cortex. *Journal of Physiology, 195*, 215–243.
Ito, M., Fujita, I., Tamura, H., & Tanaka, K. (1994). Processing of contrast polarity of visual images in inferotemporal cortex of the macaque monkey. *Cerebral Cortex, 4*(5), 499–508.
Janssen, P., Vogels, R., & Orban, G. A. (2000a). Three-dimensional shape coding in inferior temporal cortex. *Neuron, 27*(2), 385–397.
Janssen, P., Vogels, R., & Orban, G. A. (2000b). Selectivity for 3D shape that reveals distinct areas within macaque inferior temporal cortex. *Science, 288*(5473), 2054–2056.
Jones, H. E., Grieve, K. L., Wang, W., & Sillito, A. M. (2001). Surround suppression in primate V1. *Journal of Neurophysiology, 86*, 2011–2028.
Kaskan, P. M., Lu, H. D., Dillenburger, B. C., Kaas, J. H., & Roe, A. W. (2008). The organization of orientation-selective, luminance-change and binocular-preference domains in the second (V2) and third (V3) visual areas of new

world owl monkeys as revealed by intrinsic signal optical imaging. *Cerebral Cortex, 1*, 1–10. doi:10.1093/cercor/bhn178.
Keeble, D. R. T., & Hess, R. F. (1999). Discriminating local continuity in curved figures. *Vision Research, 39*, 3287–3299.
Kingdom, F. A. A., Field, D. J., & Olmos, A. (2007). Does spatial invariance result from insensitivity to change. *Journal of Vision, 7*(14), 1–13.
Kingdom, F. A. A., & Prins, N. (2005). Different mechanisms encode the shapes of contours and contour textures. *Journal of Vision, 5*, 464 [Abstract].
Kingdom, F. A. A., & Prins, N. (2009). Texture-surround suppression on contour shape coding in human vision. *Neuroreport, 20*, 5–8.
Knierim, J. J., & van Essen, D. C. (1992). Neuronal responses to static texture patterns in area V1 of the alert macaque monkey. *Journal of Neurophysiology, 67*, 961–980.
Kobatake, E., & Tanaka, K. (1994). Neuronal selectivities to complex object features in the ventral visual pathway of the macaque cerebral cortex. *Journal of Neurophysiology, 71*(3), 856–867.
Koenderink, J. J., & Richards, W. (1988). Two-dimensional curvature operators. *Journal of the Optical Society of America A, 5*, 1136–1141.
Kramer, D., & Fahle, M. (1996). A simple mechanism for detecting low curvatures. *Vision Research, 36*(10), 1411–1419.
Levi, D. M., & Klein, S. A. (2000). Seeing circles: What limits shape perception? *Vision Research, 40*(17), 2329–2339.
Levitt, J. B., & Lund, J. S. (1997). Contrast dependence of contextual effects in primate visual cortex. *Nature, 387*, 73–76.
Maunsell, J. H., & van Essen, D. C. (1983). Functional properties of neurons in middle temporal visual area of the macaque monkey. II. Binocular interactions and sensitivity to binocular disparity. *Journal of Neurophysiology, 49*(5), 1148–1167.
Moulden, B. (1980). After-effects and the integration of patterns of neural activity within a channel. *Philosophical Transactions of the Royal Society of London Series, B, 290*, 39–55.
Moulden, B., Patterson, R., & Swanson, M. (1998). The retinal image, ocularity and cyclopean vision. In G. Mather, F. Verstraten, & S. Anstis (Eds.), *The motion aftereffect: A modern perspective G* (pp. 57–84). Cambridge, MA: MIT Press.
Nelson, J. I., & Frost, B. J. (1978). Orientation-selective inhibition from outside the classic receptive field. *Brain Research, 139*, 359–365.
Nishida, S., & Ashida, H. (2000). A hierarchical structure of motion system revealed by interocular transfer of motion aftereffects. *Vision Research, 40*(3), 265–278.
Nishida, S., & Ashida, H. (2001). A motion aftereffect seen more strongly by the non adapted eye: Evidence of multistage adaptation in visual motion processing. *Vision Research, 41*, 561–570.
Nishida, S., Ashida, H., & Sato, T. (1994). Complete interocular transfer of motion aftereffect with flickering test. *Vision Research, 34*, 2707–2716.
Nothdurft, H. C., Gallant, J. L., & van Essen, D. C. (1999). Response modulation by texture surround in primate area V1: Correlates of "popout" under anesthesia. *Visual Neuroscience, 16*, 15–34.
Paradiso, M. A., Shimojo, S., & Nakayama, K. (1989). Subjective contours, tilt after-effects, and visual cortical organization. *Vision Research, 29*(9), 1205–1213.
Pasupathy, A., & Connor, C. E. (1999). Responses to contour features in macaque area V4. *Journal of Neurophysiology, 82*(5), 2490–2502.
Pasupathy, A., & Connor, C. E. (2001). Shape representation in area V4: Position-specific tuning for boundary conformation. *Journal of Neurophysiology, 86*(5), 2505–2519.
Pasupathy, A., & Connor, C. E. (2002). Population coding of shape in area V4. *Nature Neuroscience, 5*(12), 1332–1338.
Peterhans, E., & von der Heydt, R. (1993). Functional organization of area V2 in the alert macaque. *European Journal of Neuroscience, 5*(5), 509–524.
Petkov, N., & Westenberg, M. A. (2003). Suppression of contour perception by band-limited noise and its relation to non-classical receptive field inhibition. *Biological Cybernetics, 88*, 236–246.
Poggio, G. F., & Fischer, B. (1977). Binocular interaction and depth sensitivity in striate and prestriate cortex of behaving rhesus monkey. *Journal of Neurophysiology, 40*(6), 1392–1405.
Poirier, F. J., & Wilson, H. R. (2006). A biological plausible model of human radial frequency perception. *Vision Research, 46*(15), 2443–2455.
Prince, S. J., Cumming, B. G., & Parker, A. J. (2002a). Range and mechanism of encoding of horizontal disparity in macaque V1. *Journal of Neurophysiology, 87*, 209–221.
Prince, S. J., Pointon, A. D., Cumming, B. G., & Parker, A. J. (2002b). Quantitative analysis of the responses of V1 neurons to horizontal disparity in dynamic random-dot stereograms. *Journal of Neurophysiology, 87*, 191–208.
Raymond, J. E. (1993). Complete inter-ocular transfer of motion adaptation effects. *Vision Research, 33*, 1865–1870.
Regan, D., & Hamstra, S. J. (1992). Shape discrimination and the judgment of perfect symmetry: Dissociation of shape from size. *Vision Research, 32*(10), 1845–1864.
Roy, J. P., Komatsu, H., & Wurtz, R. H. (1992). Disparity sensitivity of neurons in monkey extrastriate area MST. *Journal of Neuroscience, 12*(7), 2478–2492.
Shipp, S., & Zeki, S. (2002). The functional organization of area V2. II. The impact of stripes on visual topography. *Visual Neuroscience, 19*(2), 211–231.
Steiner, V., Blake, R., & Rose, D. (1994). Interocular transfer of expansion, rotation and translation motion aftereffects. *Perception, 23*, 1197–1202.
Suzuki, S. (2001). Attention-dependent brief adaptation to contour orientation: A high-level aftereffect for convexity? *Vision Research, 41*, 3883–3902.
Suzuki, S. (2003). Attentional selection of overlapped shapes: A study using brief shape aftereffects. *Vision Research, 43*, 549–561.
Suzuki, S., & Cavanagh, P. (1998). A shape-contrast effect for briefly presented stimuli. *Journal of Experimental Psychology: Human Perception and Performance, 24*(5), 1315–1341.
Tanaka, K. (1996). Inferotemporal cortex and object vision. *Annual Review of Neuroscience, 19*, 109–139.
Tanaka, H., Uka, T., Yoshiyama, K., Kato, M., & Fijita, I. (2001). Processing of shape defined by disparity in monkey inferior temporal cortex. *Journal of Neurophysiology, 85*(2), 735–744.
Tyler, C. W. (1973). Periodic vernier acuity. *Journal of Physiology, 228*(3), 637–647.
Uka, T., Tanaka, H., Yoshiyama, K., Kato, M., & Fujita, I. (2000). Disparity selectivity of neurons in monkey inferior temporal cortex. *Journal of Neurophysiology, 84*, 120–132.
Vreven, D., & Berge, J. (2007). Detecting structure in glass patterns: An interocular transfer study. *Perception, 36*(12), 1769–1778.
Wallis, G., & Rolls, E. (1997). Invariant face and object recognition in the visual system. *Progress in Neurobiology, 51*, 167–194.
Watanabe, M., Tanaka, H., Uka, T., & Fujita, I. (2002). Disparity-selective neurons in area V4 of macaque monkeys. *Journal of Neurophysiology, 87*, 1960–1973.
Wilson, H. R. (1985). Discrimination of contour curvature: Data and theory. *Journal of the Optical Society of America A, 2*(7), 1191–1199.
Wilson, H. R. (1991). Pattern discrimination, visual filters and spatial sampling irregularity. In M. S. Landy & J. A. Movshon (Eds.), *Computational models of visual processing*. Cambridge, MA: MIT Press.
Wilson, H. R., & Richards, W. A. (1989). Mechanisms of contour curvature discrimination. *Journal of the Optical Society of America A, 6*, 106–115.
Wiskott, L. (2004). How does the visual system achieve shift and size invariance? In J. L. van Hemmen & T. J. Sejnowski (Eds.), *Problems in systems neuroscience*. New York: Oxford University Press.
Yao, H., & Li, C.-Y. (2002). Clustered organization of neurons with similar extra-receptive field properties in the primary visual cortex. *Neuron, 35*, 547–553.
Zeki, S. M. (1978). Uniformity and diversity of structure and function in rhesus monkey prestriate visual cortex. *Journal of Physiology, 277*, 273–290 [London].